Tellus (2004), 56A, 218–228
Printed in UK. All rights reserved

TELLUS

Blocking prediction in an ensemble forecasting system

By THORSTEN MAURITSEN* and ERLAND KÄLLÉN, *Department of Meteorology, Stockholm University, S-106 91 Stockholm, Sweden*

(Manuscript received 3 March 2003; in final form 21 November 2003)

ABSTRACT

The predictability of the atmospheric blocking phenomenon is investigated using the output of the high-resolution ensemble prediction system of the European Centre for Medium-Range Weather Forecasts.

The output from the model is analysed using an objective blocking index. This is compared with the theory of Charney and DeVore that blocking is a large-scale non-linear phenomenon. A consequence of the non-linearity is that in some cases multiple quasi-stationary atmospheric states can exist for the same set of boundary conditions.

It is found that the model in general produces too few blocks. Good agreement is found between the models lacking ability to predict blocking frequency and the systematic errors of 500-hPa geopotential height. It is found that there exists a limit, in the middle of the medium range, beyond which forecasts of blocking onset should be considered as probabilistic rather than dynamical. Inspection of individual blocking events adds new support to the idea that atmospheric blocking can be explained using the Charney–DeVore model.

1. Introduction

Atmospheric blocking is a dominating characteristic feature of large-scale, stationary flow patterns in the mid-latitudes. Both the definition of blocked flow and proposed dynamical theories have received much attention in the past. In the present study we investigate the ability of an ensemble prediction system to forecast blocking in the medium range. The ensemble system provides us with a large number of forecasts of the same events, which can be considered within the initial uncertainty. This allows us to closely study the dynamical behaviour of the model. We compare this with the theory of Charney and DeVore (1979).

Some of the first systematic studies on the large-scale atmospheric blocking phenomenon were carried out by Rex (1950a,b, 1951). These were preceded by several observational studies of the phenomenon; see, for example, Berggren et al. (1949) and references therein. Using 500-hPa geopotential maps, Rex identified a recurrent atmospheric flow pattern and defined a blocking pattern using subjective criteria. He found that the presence of the large-scale blocking high had a major impact on regional temperatures and precipitation.

Wallace and Gutzler (1981) used point correlations in 500-hPa geopotential height analysis to identify tele-connections. They found that the most prominent patterns exhibited several centres of action, resembling standing Rossby waves on the sphere. Dole and Gordon (1983) inferred a criterion to identify persistent anomalies, also using Northern Hemisphere (NH) mid-tropospheric weather maps. Lejenäs and Økland (1983) designed a criterion to identify the longitudinal distribution of blocking highs. They required that the 500-hPa geopotential height should be higher at 60N latitude than at 40N latitude at a certain longitude in order for it to be blocked. We shall call this index the Lejenäs–Økland index. In all three studies it was found, using widely different methods, that the most prominent, persistent and blocked patterns are found in the Pacific (PAC) and European–Atlantic (EA) areas.

A possible explanation for the blocking phenomenon was proposed by Charney and DeVore (1979). They used a simple barotropic channel model to show that multiple stationary non-linear solutions are possible in the largest scales for reasonable parameters. Many later studies have addressed the question as to whether the atmospheric behaviour can be explained by this theory. We return to this in more detail after having described the Charney–DeVore model in Section 2.

The purpose of an ensemble prediction system is to approximate the atmospheric probability distribution function for a future atmospheric state given an uncertainty in the analysis and the prediction. Following Molteni et al. (1996) this is the case if:

(a) the sample of initial states provides a realistic estimate of the probability distribution of analysis errors; and

(b) the phase-space trajectories computed by the numerical model are good approximations of atmospheric trajectories.

*Corresponding author.
e-mail: thorsten@misu.su.se

Most work on ensembles has been focused on part (a), likely because the primary use of the systems has been to estimate the errors of short-range forecasts during data assimilation. For computational reasons we are limited to use a small subset of the, in principle, infinite-dimensional initial uncertainty. Here, the use of singular vectors or breeding vectors provides a good estimate of errors for short-range forecasts. With the increasing interest in medium-range, seasonal and even climatological forecasts, part (b) becomes ever more important. This means that not only should the prediction system have similar climatology, but it should also dynamically resemble the real atmosphere. In the case of atmospheric blocking we expect the perfect model to produce blockings with similar dynamical and statistical behaviour, that is the same frequencies, typical lengths, size, geographical distribution, etc.

Several studies have been conducted on the issue of blocking predictability. Tibaldi and Molteni (1990) used the operational forecasts from the European Centre for Medium-Range Weather Forecasts (ECMWF) to investigate the model's ability to predict blockings. Investigating seven winters of data using the Lejenäs–Økland index, they found that in the medium range the model severely underestimated blocking frequency. Blocking onset has been found to be poorly represented if it occurs more than a few days into the forecast. These results were confirmed in later studies by Tibaldi et al. (1994, 1995) using the same methods but for larger data sets.

During the Atmospheric Model Intercomparison Project (AMIP), 15 general circulation models were integrated for 10 yr. D'Andrea et al. (1998) investigated the output of the models using the Lejenäs–Økland index. All models produced too few blockings. Of all the models in the test, the ECMWF model was among the better, however by no means the best. For instance, the UK Meteorological Office (UKMO), ECHAM, National Center for Atmospheric Research (NCAR) and National Meteorological Center (NMC) models were superior to the ECMWF model with respect to reproducing the annual cycle of blocking frequency. All the above model studies use previous versions of the ECMWF forecasting system, while our results refer to a more recent one. A direct comparison is therefore difficult to make, but we may infer whether the model has improved or if the deficiencies found in earlier studies still remain.

First, we describe the Charney–DeVore model and introduce the concept of a pseudo-potential in conjunction with this model. Next, in Section 3, we define an objective blocking criterion, following Lejenäs and Økland (1983). In Section 4 we present the results from the ensemble prediction system, using both traditional error measures and the objective blocking index. In Section 5 we inspect the forecasts of individual blocking events and interpret the dynamical behaviour of the model in terms of the Charney–DeVore model. Finally, we sum up the results in Section 6.

2. A pseudo-potential approach to multiple equilibria

An analytical model, which can be used to explain the atmospheric blocking phenomenon, was developed by Charney and DeVore (1979) in the late 1970s. They used a simple barotropic β-plane channel model with a rigid lid to show that more than one stable, steady solution was possible for the same boundary conditions. Dissipation is added in the form of a vorticity sink of the Ekman type:

$$\frac{\mathrm{D}}{\mathrm{D}t}\left[\nabla^2\psi + \beta y + f_0\frac{h}{H}\right] = F - r\nabla^2\psi. \tag{1}$$

Here, D/Dt is the Lagrangian time derivative, ψ is the stream function, h is the height of the topography, H is the height of the atmosphere, $r = \tau^{-1}$ is the inverse of the Ekman pumping e-folding time, f_0 is the Coriolis parameter at some central latitude, β is the variation of the Coriolis parameter in the y-direction and F is a forcing term. The channel is cyclic in the x-direction at a length L_x and has walls at $y = 0$ and at $y = L_y$.

This infinite-dimensional dynamical system can be reduced to a one-dimensional system in the mean zonal wind, $\bar{u}$. The flow is divided into a mean flow component and two orthogonal spatial spectral components with the same wavenumbers, k and l. The topography is also chosen as a single spectral component with the same wavenumbers. Zonal averaging and integration in y is performed following Holton (1992). The non-linear higher-order terms are retained. We can define an averaged forcing as a linear relaxation towards a prescribed zonal flow

$$\int \bar{F}\,\mathrm{d}y \equiv -\kappa(U_\mathrm{e} - \bar{u}), \tag{2}$$

where U_e is the steady solution for $\bar{u}$ in the absence of topography. Furthermore, the effect of topographic wave drag on the zonal flow can be defined as

$$\begin{aligned} D(\bar{u}) &\equiv -\frac{f_0}{H}(\overline{v'h}) \\ &= \left(\frac{r f_0 \hat{h}^2}{H^2}\right)\frac{K^2}{\bar{u}}\frac{\cos^2(ly)}{(K^2 - (\beta/\bar{u}))^2 + (rK^2/k\bar{u})^2}, \end{aligned} \tag{3}$$

which owes its non-linearity to the resonance of standing Rossby waves over periodic topography near $\bar{u} = \beta/K^2$. Here k and l are zonal and meridional wavenumbers, $K^2 \equiv k^2 + l^2$ and $\hat{h}$ is the topography amplitude. With these definitions we obtain a time evolution equation for the mean zonal wind:

$$\frac{\mathrm{d}\bar{u}}{\mathrm{d}t} = \kappa(U_\mathrm{e} - \bar{u}) - D(\bar{u}). \tag{4}$$

Analytical solutions to eq. (4) are found when the forcing and friction terms equal each other. A neat way to infer the stability of these fixpoints with respect to small perturbations is to define

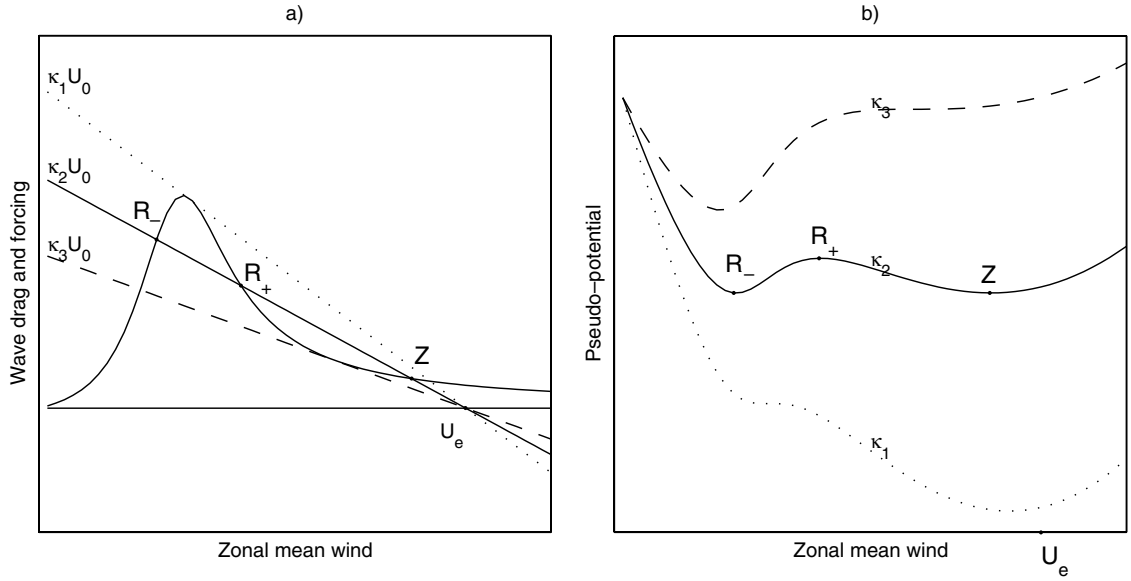

Fig. 1. Graphic illustration of eq. (4). In (a) the form drag term is plotted as a thick line, while three examples of the forcing term, which depends only on κ, are plotted with thinner lines. Stationary solutions are at the intersections between the forcing and the drag. (b) The pseudo-potentials for the values of κ in (a) are plotted. Zonal wavenumber k is everywhere set to $10/(\pi L_x)$ and meridional wavenumber l is set to $1/(\pi L_y)$. The central latitude, λ_0, was 45N, the width of the channel was $L_y = 5000$ km, the length of the channel was $a\cos(\lambda_0)$ and $r = (5\text{ d})^{-1}$.

and calculate the pseudo-potential, V:

$$-\frac{\mathrm{d}V}{\mathrm{d}\bar{u}} \equiv \frac{\mathrm{d}\bar{u}}{\mathrm{d}t}. \tag{5}$$

At the fixpoints of eq. (4), V will be either a local maximum or a local minimum, if the right-hand side is well behaved. If V is a local maximum, the fixpoint is unstable and if it is a local minimum the fixpoint is stable.

In Fig. 1b we see how different values of κ can lead to different pseudo-potentials. For the case of κ_2 the system has three stationary solutions of which two are stable, R_- and Z. Two head-to-head saddle-node bifurcations occur at κ_1 and κ_3 towards a single stable solution, Z and R_- respectively. We note that the system is not chaotic. To make the system transfer between equilibrium states, more wave components need to be included.

Bifurcation theory has later been applied to more complex models by several authors, including Källén (1981), Reinhold and Pierrehumbert (1982) and Legras and Ghil (1985), finding multiple stationary states in models of varying complexity. Itoh and Kimoto (1996) found that the roles of multiple stationary states are replaced with multiple stable attractors in a high-resolution model for a fairly wide range of input parameters. When the parameters are changed in order to generate more activity in the system a transition occurs. The former stable attractors are no longer stable, but their fingerprints remain as ghosts or ruins of the former attractors in phase-space. Solutions reside for a fairly long time in the vicinity of these quasi-stable states interrupted by swift transitions between them. These transitions in a double-well pseudo-potential have characteristic time-scales of the subscale motions or noise responsible for the transitions (Ditlevsen, 1999).

In the simple channel model, Rossby waves are confined to the model domain by artificial focusing by the channel walls, allowing them to amplify. The introduction of spherical geometry makes this questionable because Rossby waves disperse out of the mid-latitudes along great circles (Hoskins and Karoly, 1981; Källén, 1985). However, the large-scale structure of the atmosphere, with westerlies in the mid-latitudes capped to the north and south by easterlies, allows for focusing of Rossby waves, thus creating the possibility for topographically generated resonance (Held, 1983; Yang et al., 1997; Pavan et al., 2000).

Recent model results indicate that there is an important connection between the planetary scale blocking phenomenon and the synoptic scale transient eddies in the formation, maintenance and breakdown of blocking through wave to wave non-linear interaction (Chen and Juang, 1992; Michelangeli and Vautard, 1998). This upscale cascade can have important consequences for the limitations of numerical prediction of blocking events. In an ensemble prediction system, the uncertainties in the transient eddies are treated through the use of singular or breeding vectors (Buizza and Palmer, 1995; Hoskins et al., 2000).

3. Objective blocking criteria

A commonly used objective blocking index was first suggested by Lejenäs and Økland (1983). The simple idea was to require the geopotential to be larger at some high latitude than at some lower latitude for the flow to be blocked. This implies that, on

average, the flow between the two latitudes must be easterly. Later, the idea was modified in several studies of atmospheric blocking (Tibaldi and Molteni, 1990; Tibaldi et al., 1994, 1995; D'Andrea et al., 1998; Pavan et al., 2000). We shall use the original index with later modifications following Tibaldi and Molteni (1990) and D'Andrea et al. (1998), slightly modified to our data sets.

We consider whether or not a certain longitude is blocked. If $Z(\phi)$ is the geopotential as a function of latitude, then we define the geopotential height gradients *GHGS* and *GHGN* as

$$GHGS \equiv \frac{Z(\phi_0) - Z(\phi_S)}{\phi_0 - \phi_S}$$

$$GHGN \equiv \frac{Z(\phi_N) - Z(\phi_0)}{\phi_N - \phi_0},$$

where

$$\phi_S = 40^\circ N + \Delta$$

$$\phi_0 = 60^\circ N + \Delta$$

$$\phi_N = 80^\circ N + \Delta$$

$$\Delta = -5^\circ, -2.5^\circ, 0, 2.5^\circ, 5^\circ.$$

Then the longitude is blocked if, for at least one Δ, the following requirements are met:

(1) $GHGS > 0$,
(2) $GHGN < -5$ m/degree latitude,
(3) $\sum_{\lambda=-7.5^\circ}^{7.5^\circ} GHGS(\lambda) > 0$.

Here, the sum is over the longitude, λ, of interest and the six adjacent longitude segments of 2.5°. Conditions (1) and (3) are identical to those of Lejenäs and Økland (1983), whereas the use of Δ is due to Tibaldi and Molteni (1990) and condition (2) is due to D'Andrea et al. (1998).

Condition (1) is by far the most important. It states that, in some interval in the mid-latitudes, average geostrophic winds should be easterly as opposed to the climatological westerly winds. Requirement (2) states that some westerly flow should go north around the mid-latitudinal block. Therefore, the ridge cannot extend all the way to the North Pole. This is important in the PAC. Requirement (3) simply states that the block should have a certain horizontal extent in order to eliminate synoptic scale low-latitude cyclonic systems. Note how this interpretation of the objective criteria corresponds to several points in the subjective criteria of Rex (1950a,b, 1951).

In Fig. 2 the longitudinal dependency of blocking frequency is plotted for the National Center for Environmental Predictions (NCEP) 1948–2001 daily reanalysis of 500-hPa geopotential height. The distribution exhibits two distinct maxima. From these two maxima, following D'Andrea et al. (1998) closely, we shall define the sectors:

(1) EA, 25° W–40°E;
(2) PAC, 115° E–215°E.

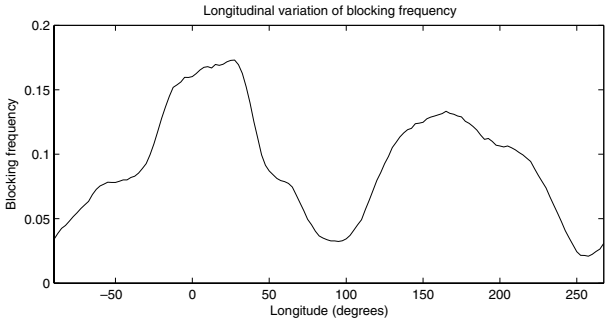

Fig. 2. Blocking frequency as a function of longitude for the NCEP reanalysis data set from 1948 to 2001. A frequency of one means that the flow is always blocked.

In Fig. 3a we plot a composite map of all blockings at Greenwich and their associated anomalies. In the latter, the seasonal variation of blockings at that specific longitude is taken into account. Note the large spatial scale and amplitude of the blocking pattern.

4. Errors in ensemble forecasts

Operational ensemble forecasts of 500-hPa geopotential height from ECMWF for the period 1 December 2000 to 28 February 2001 were used to evaluate the performance of the prediction system. Because medium-range forecasts are made for 10 d at ECMWF, the first 10 d of the period and the forecasts valid after 28 February were discarded in order for all forecasts to be valid on the same set of days. The ensemble forecasts at ECMWF consist of 50 members, which are perturbed from the analysis using singular vectors. The 80 d times the 50 ensemble members is equivalent to nearly 11 yr of single integration deterministic forecasts. However, the ensembles cannot be considered as independent in a strict statistical sense.

During this period the general circulation model used for the ensemble forecasts had a resolution called $T_L255L40$, corresponding to spectral truncation at total horizontal wavenumber 255 and 40 vertical levels. In connection with this, it should be noted that previous studies have used models with cruder resolutions, for instance truncation at wavenumber 40 in Tibaldi and Molteni (1990) and Tibaldi et al. (1994, 1995), truncation at wavenumber 42 and 19 vertical levels in D'Andrea et al. (1998) and truncation at wavenumber 63 and 31 vertical levels in Pavan et al. (2000). The data from ECMWF were received on a 2.5 × 2.5° regular grid.

4.1. Systematic and root mean square errors

It is customary to use systematic and root mean square (rms) error measures when inspecting the performance of a numerical weather prediction system (e.g. Simmons et al., 1995). We shall compare this method with the error measure of the blocking index used in the present work.

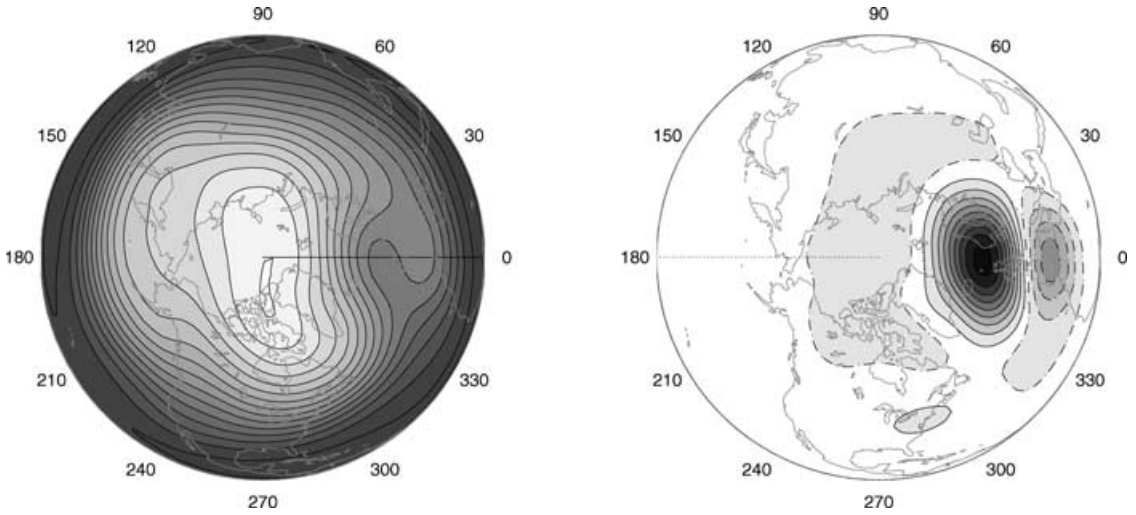

Fig. 3. Composite maps of all blockings at Greenwich in the period 1948–2001 at the 500-hPa level. The left panel shows the average over 3158 of the total 19 710 d included in the NCEP reanalysis. The contour interval is 50 geopotential metres. The right panel shows the anomaly associated with blockings at Greenwich, where the seasonal variation of blockings are taken into account. Here the contour interval is 20 geopotential metres. Dashed contours are negative. The map projection is spherical.

We can define the systematic error or bias as

$$\text{systematic error} \equiv \frac{1}{n}\sum_{i=1}^{n}\left(Z_i^{\mathrm{f}} - Z_i^{\mathrm{o}}\right), \tag{6}$$

where Z denotes geopotential height, 'f' and 'o' superscripts indicate the forecast and observation, respectively, and the sum is over n points. Similarly, the rms error measure can be defined as

$$\text{rms error} \equiv \sqrt{\frac{1}{n}\sum_{i=1}^{n}\left(Z_i^{\mathrm{f}} - Z_i^{\mathrm{o}}\right)^2}. \tag{7}$$

In Fig. 4 we see the classical behaviour of the mean rms error for the NH mid-latitudes. We see the initial development of the errors are close to exponential growth. Actually, the growth is superexponential due to the use of singular vectors for the ensembles (e.g. Trevisan et al., 2001). After a while the errors start to saturate as the variability is limited by the sizes of the model and real-world attractors. We note that the ensemble mean has remarkably better performance with respect to mean rms error than the individual ensemble members.

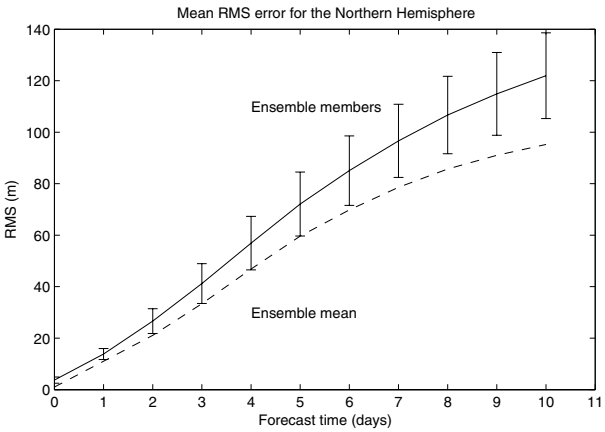

Fig. 4. Mean rms error for the NH mid-latitudes (20N to 80N). The solid line is the error of the individual ensemble members as a function of forecast time as compared to the analysis at validation time. The error bars show the spread among the members. The dashed line is the mean rms error for the ensemble mean.

In Fig. 5 the distributions of systematic and rms errors are plotted for different forecast lengths. We note that the spatial scales of the mid-latitude systematic errors resemble those of the blocking anomaly of Fig. 3 and that the maxima and minima are situated in the blocking sectors, as also found by Ferranti et al. (2002). The systematic errors found in the Tropics can be assigned to problems in model formulations (Palmer et al., 1990). The systematic errors in the mid-latitude PAC could be related to errors in blocking frequency, as we shall see in Section 4.2.

4.2. *Blocking frequency distribution*

The next natural question is how the model produced blockings are distributed in comparison with the analysis. Figure 6 plots the frequency distribution as a function of longitude for both the analysis and various forecast times. We note that the EA sector has good representation of the frequency distribution up to and including the 6-d forecast, while the model has serious trouble with the PAC sector already at day four forecasts. In the 10-d forecasts only the eastern part of the EA sector and the minima between the sectors are well represented.

This should be compared to the average blocking frequency from the NCEP reanalysis plotted in Fig. 2. We note that the winter 2000–2001 analysed blocks showed a strong anomaly in the central parts of the PAC sector, but it was otherwise to be considered normal. The 10-d forecast distribution bears some

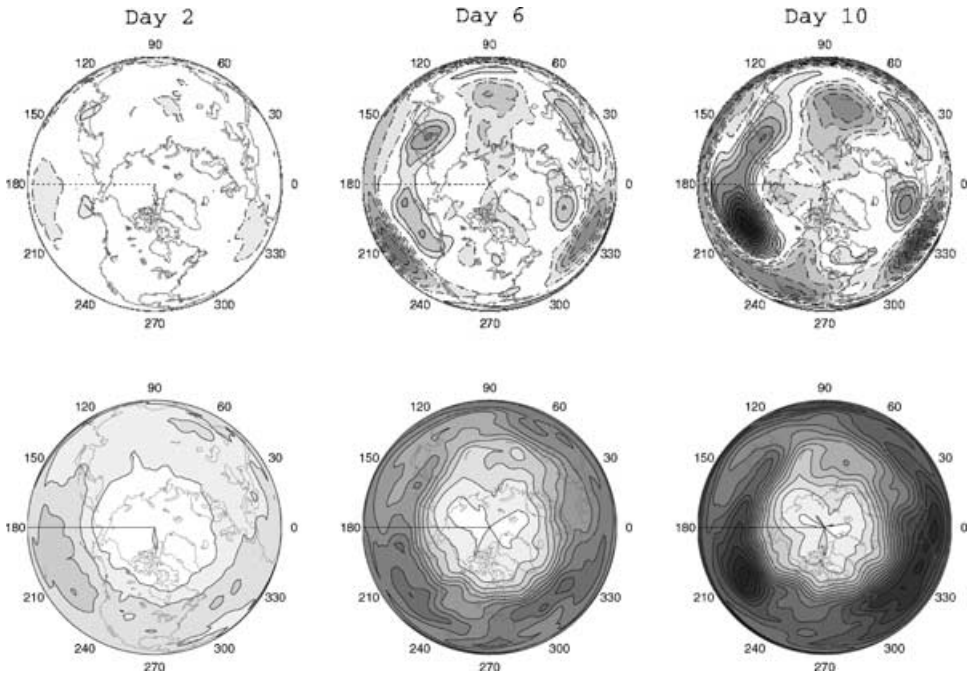

Fig. 5. Top panels show the systematic error distribution while the bottom panels show the rms error distributions for forecast days 2, 6 and 10, respectively. Positive values are plotted with a solid line whereas negative values are plotted with a dashed line. The contour interval is 10 geopotential metres.

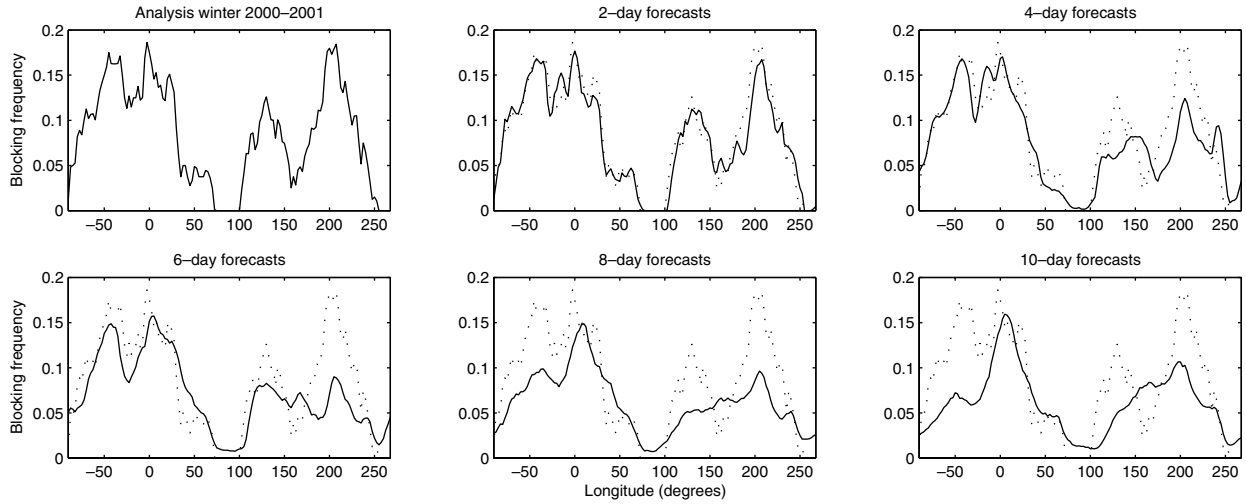

Fig. 6. Frequency distribution of blockings as a function of longitude for the analysis and different forecast lengths. In all the forecast plots the analysed blocking frequency is plotted with dotted lines for comparison. A frequency of one means that the flow is always blocked.

resemblance to the NCEP distribution. However, the amplitude is slightly lower.

We expect mid-latitude systematic errors in the 10-d forecasts to have minima and maxima where the discrepancies between analysed and predicted blocking frequency are largest. Comparison between Figs. 5 and 6 shows good agreement around 50W, 150E and 200E as well as a more vague agreement near 100E. The actual effect of errors in blocking frequency on systematic errors are expected to depend on the structure of blockings at the specific location in question.

The apparent behaviour of the model to produce too few blockings could be interpreted using the simple non-linear model of Charney and DeVore described in Section 2. Imagine that we have a situation where the atmospheric pseudo-potential looks something like the solid curve in Fig. 1b. Then let the numerical model, with which we make forecasts, have a tendency to drift towards a stronger zonal wind. This could give the model a pseudo-potential like the dotted curve. This would cause a drift away from the R_- solution, regardless of the initial conditions, explaining the deficit in blocking frequency of the forecasts.

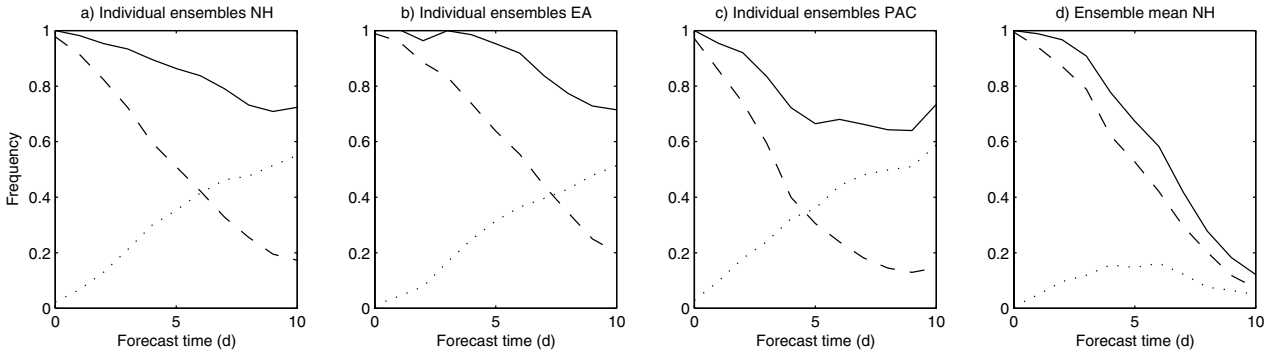

Fig. 7. Blocking prediction performance as a function of forecasting time for the ECMWF ensemble prediction system for the winter 2000–2001. Dashed lines show the frequency of correctly forecasted blocks, dotted lines show the blocks forecasted by the model which did not appear in the analysis, and the solid lines show the total blocking frequency. All values are normalized by the initial total blocking frequency in each case.

4.3. Blocking predictability

A very simple approach to the problem of investigating the ECMWF models ability to predict blockings is to count the correct and incorrect blockings as they appear in the forecasts. By a blocking we mean a blocked longitude segment on the retrieval grid.

4.3.1. Individual members. First, we will inspect the ability of the individual ensemble members to correctly predict atmospheric blocking. Figures 7a–c show these statistics for the NH, the EA sector and the PAC.

We see how correctly forecasted blocks decrease for longer forecasting times, whereas incorrectly forecasted blockings increase. Initially we could expect errors to grow close to exponentially. Later, this growth should saturate due to the limited total variability of the system. The saturation level would depend on both the atmosphere's and the models' likelihood of producing a block in each longitude. Even beyond the limits of predictability, the model could be right simply by chance. We note how the model performs better in the EA sector than in the PAC sector. In the PAC sector it looks as if saturation is reached at about 8-d forecasts, whereas in the EA no saturation is yet apparent at the end of the forecasts.

Along with the correct and incorrect blocks, the sum of the two is plotted. We see that overall the model predicts a decreasing number of blocks. At the 10-d forecast, the number of blocks has decreased by some 30 per cent. This should be compared with the 50 per cent decrease found by Tibaldi and Molteni (1990) from forecasts by the ECMWF model during the winters 1980–81 to 1986–87. However, the number of correctly predicted blockings has not improved since then. For the PAC, this decrease appears to be much more rapid than for the EA. This is in line with the previously shown results.

4.3.2. Ensemble mean.. As can be seen in Fig. 4 the ensemble means have better performance than the individual members with respect to the rms error measure. Therefore, it would be interesting to see the performance with respect to predicting atmospheric blocking.

Figure 7d shows the blocking prediction statistics for the ensemble mean forecast. Qualitatively, this differs very much from that in Fig. 7a. The total number of blocks decreases rapidly in the medium range, beyond two to three days of forecasting, primarily because almost no incorrectly predicted blocks appear. Also the number of correct blocks is half of that in Fig. 7a at day 10 forecasts.

This can be interpreted in terms of the multiple quasi-stationary states in the Charney–DeVore model. The individual ensembles can be in either of these states. If we take a weighted average of these states, then this average will not necessarily resemble any of the states. Therefore, it can be that the ensemble average is not representative for any of the persistent flow regimes. In other words, it has no physical relevance.

5. Dynamics of ensemble blocking predictions

In assessing the model performance we can take the simple view of Section 4.3 that blocks are either correctly or incorrectly predicted at specific longitudes. A more delicate view of things would be to ask whether the blocks are correctly placed in space and time. As we shall see, this can provide important information on how to interpret the forecasts.

Each member of the ensemble prognosis system predicts blocked or non-blocked flow for each longitude 10 d ahead. Thus, we have three degrees of freedom: longitude, validation time and forecast time. From our data set of several subsequent ensemble forecasts, we can construct the ensemble blocking density, defined as the number of blocked ensemble members. From this density we can inspect the model's ability to position the blockings correctly in space and time.

As we are dealing with a chaotic dynamical system, we expect to find some certain characteristics in the ensemble blocking density. It can be shown for chaotic systems that small errors develop exponentially initially. After some time, the error growth is limited by the total variability. The ensemble is intended to

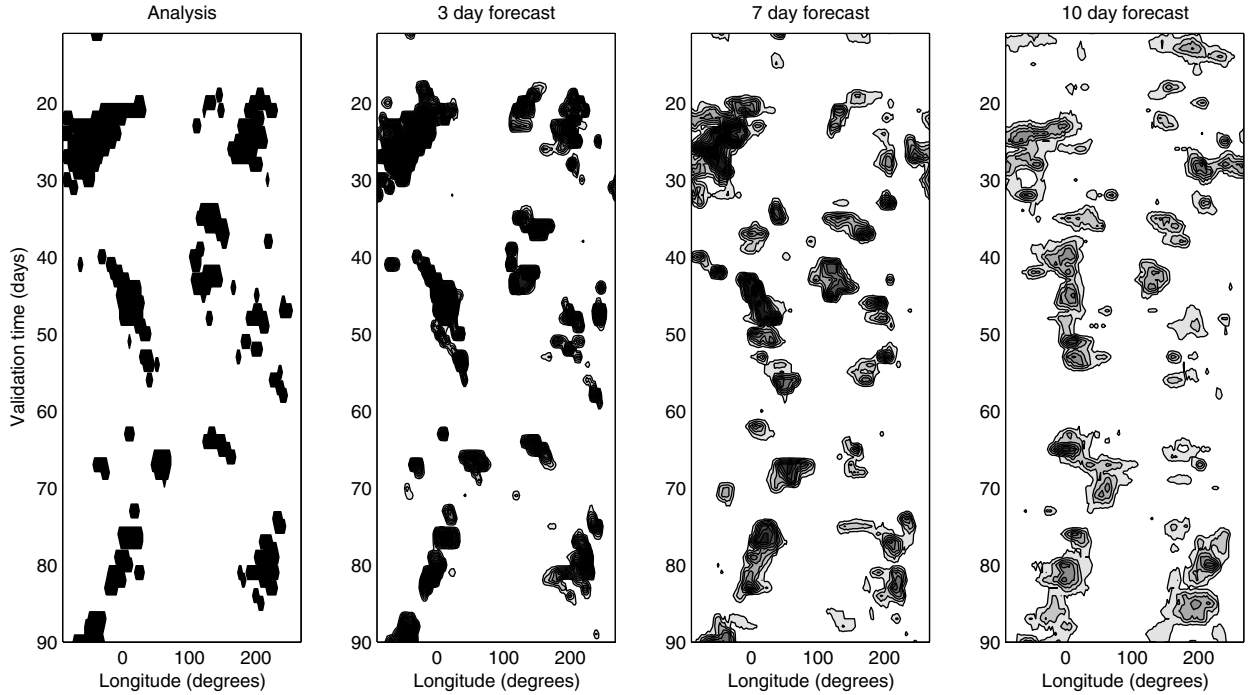

Fig. 8. Analysed and forecasted blockings for the entire period as a function of longitude and validation time. The contour line interval is 0.1 or 5 of the total of 50 ensemble members, and thus black corresponds to 45 or more blocked ensemble members.

represent the initial uncertainty. Thus, at some stage we expect this initial uncertainty to cause some ensemble members to be blocked while others are not. This uncertainty should cause the ensemble blocking density to be smeared out in both space and time for longer forecast times.

In Fig. 8 we have shown the distribution of ensemble blocking density for the analysis and three different forecast times. At first glance most events are well captured throughout the forecast. This applies especially to those of the EA sector. The longitudinal positioning of blocking events is found to be quite good. In the PAC, the model seems to have more trouble capturing the distribution of the analysis. The smearing, mentioned above, is hardly evident in the 3-d forecasts, but becomes pronounced in the 7-d and 10-d forecasts.

Closer inspection reveals that in many cases the onset and decay of the blocking events are postponed towards later validation days for increasing forecast length. Figure 9 shows an example of an onset of a blocked flow. In this plot the onset validation day has been set to 1. If the forecast were to be perfect the lower half would be completely black and the upper half white. A forecast starting from a particular initial state, follows a sloping line forming an angle of 45° with the horizontal axis, see Fig. 9. Here we have plotted three lines indicating forecasts based on analysis made five, six and seven days before the blocking onset, respectively. Note the dramatic increase in ensemble blocking frequency from 0.1 to 0.3 in the forecasts originating seven days before the onset to 0.7 to 1.0 in the forecasts based on analysis five days before.

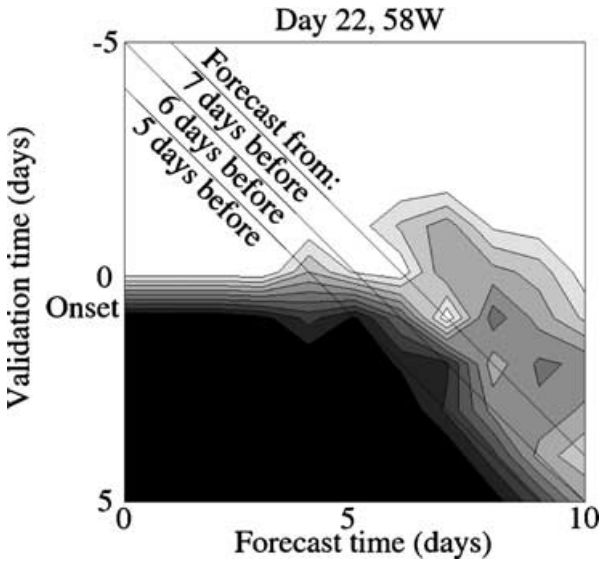

Fig. 9. An example of an ensemble forecast of a blocking onset on day 22 and at 58W of Fig. 8. The plot shows ensemble blocking density. It is normalized such that blocking onset takes place at validation day one. The blocking frequency contour interval is 0.1 as in Fig. 8. Three lines corresponding to forecasts based on analysis five, six and seven days before the blocking onset are shown.

Figure 10 shows all onsets of blocked flow that lasted four days or longer and had a longitudinal extent of more than 10°. Here, it can be seen that in almost all the cases the forecasts are indeed close to perfect in terms of blocking prediction for the first

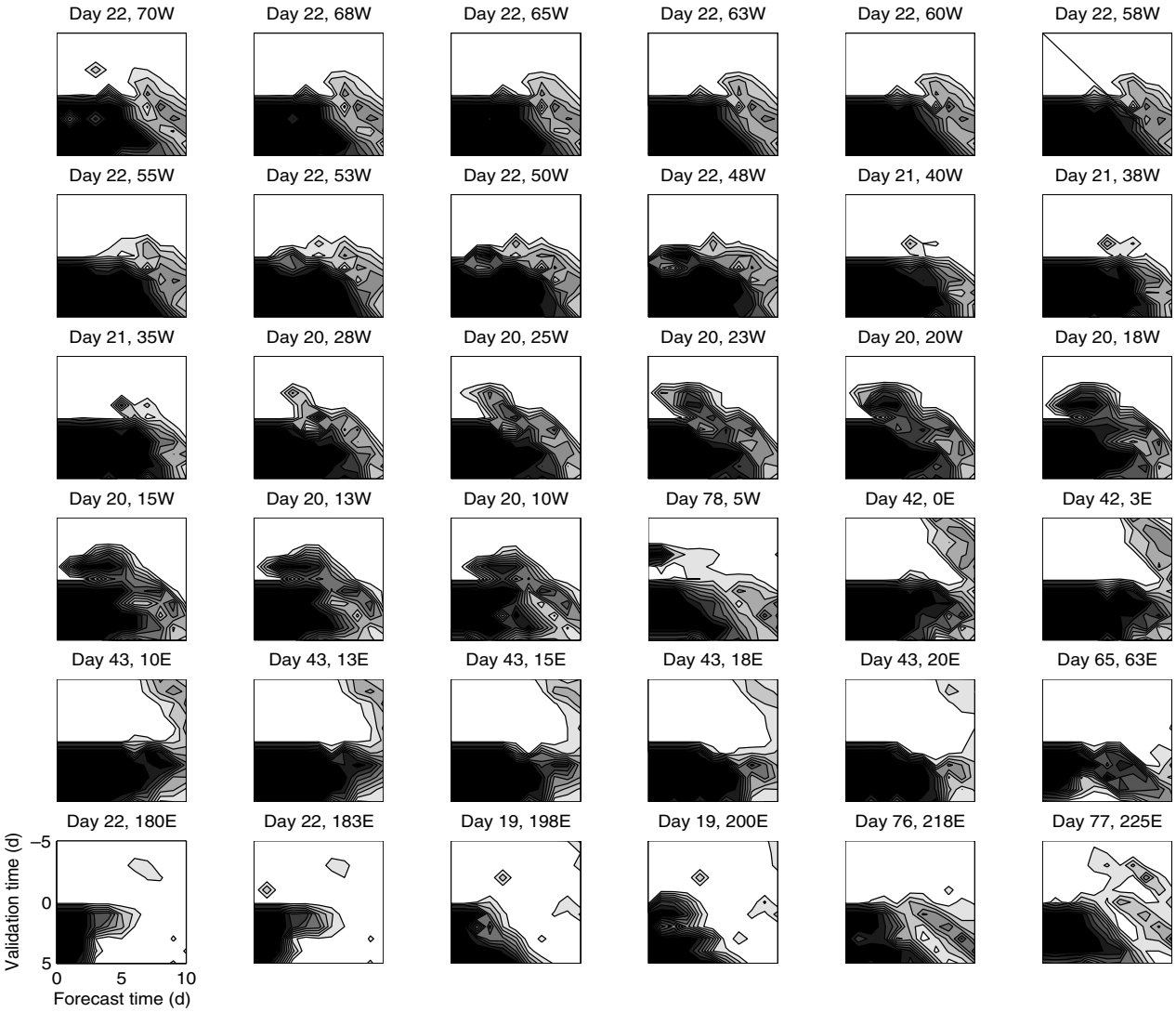

Fig. 10. All major blocking onsets for the entire period, lasting for at least four days and with a geographical size of more than 10° longitude. See Fig. 9 for explanations of labels and contour intervals. All plots are titled with validation day and longitude corresponding to Fig. 8.

three to five days. Beyond this limit some smearing takes place. However, it is not completely random smearing. In fact, many of the contour lines seem to have a tilt of approximately 45° to the horizontal. This implies that, after a certain validation date, ensemble forecasts will switch from being dominated by a zonal regime throughout the forecast into evolving towards a blocked flow. Note that the switch takes place at a certain date, not after a particular length of the forecast. Also, note that this behaviour relates to the majority of the ensemble, not just to individual members. This time lag of blocked flow onset in the medium-range forecasts could be partly responsible for the rapid error growth in blocking predictions seen in Fig. 7. In other words, there is a general increase in rms error for individual ensemble members, but a systematic shift in blocked versus non-blocked flow occurrences.

If the blocking mechanism were dominated by linear processes, we would instead have found that forecasts beyond a certain forecast range would either enter or leave a blocked flow regime. The reasoning behind this is as follows. In linear theory, it is assumed that slow changes in the background state, under which the flow is linearized, uniquely determine the asymptotic state. In terms of the pseudo-potential, introduced in Section 2, this corresponds to a single minimum. All initial states will sooner or later end up in the vicinity of that minimum. A change in background conditions will move the position of this minimum. Examples of background conditions are the meridional structure of the zonal mean flow, and the strength of the equator-to-pole temperature gradient that determines the forcing of the zonal mean flow. It is the assumption that the time-scale of changes in the background conditions is long compared to the

characteristic time-scale of changes in the large-scale, synoptic flow.

In non-linear theory, it is possible to have more than one asymptotic state for a given set of background conditions. We can think of this as a system governed by a pseudo-potential with more than one minimum. The asymptotic state, which is picked by the system, depends solely on the initial state.

An ensemble system deals with the analysis uncertainty by perturbing the initial conditions. During the forecast the spread among the ensemble members increase. When they are sufficiently close, they are likely to approach the same asymptotic state. As the spread increases, it becomes increasingly uncertain towards which of the possible states the individual ensemble members will move. This could be what happens beyond the three to five day forecast limit, when only a small fraction of members seem to enter the blocked flow state.

6. Conclusions

We have investigated the output of an ensemble prediction system using an objective blocking criterion. The results are compared with the theory of Charney and DeVore (1979). This theory suggests that the atmosphere can be in either of two possible stable stationary states. We have shown that this corresponds to motion in a double-well pseudo-potential. Once the system has entered the vicinity of one of the stable states it is reluctant to leave, due to the potential barrier between the states.

There is good agreement between mid-latitude rms errors in medium-range weather forecasts and the general blocking intensity. This implies that a large part of total variability is due to blockings. The comparisons between mid-latitude systematic errors and the specific blocking frequency errors as a function of longitude for the winter period at hand also agree rather well. It was shown that the model at hand produced on average some 30 per cent less blockings than were present in the analysis. This indicates that not only do blockings comprise a large fraction of total forecast error in the medium range, but the inability of the model to produce a realistic blocking frequency can cause systematic errors in the mid-latitudes. This is, however, an improvement compared to the 50 per cent decrease Tibaldi and Molteni (1990) found for earlier versions of the ECMWF model.

Considering the Charney–DeVore model, this implies that systematic errors in the mid-latitudes should be considered as non-local in nature. Errors that appear in the mid-latitudes are not necessarily due to faulty model formulations at that specific location. Instead, for instance, the properties of a wave-guide governing the propagation of large-scale waves in the model might be different from the real atmosphere, or possibly the propagation of waves into the stratosphere could be erroneous.

While individual ensemble members might be useful to predict blockings, we have shown that the ensemble mean gives unrealistic results. If the atmosphere is a system with two quasi-stationary states, then taking the average of an ensemble, of which part is in one state and the rest is in the other, gives a state which is neither one nor the other. In other words, it is not physically relevant.

Inspection of the individual blocking events supports the Charney–DeVore theory. We have shown that the model predicts the longitudinal position of blockings quite well. The reason for this could be that blocking is a phenomenon with preferred geographical positions, and that the model captures this behaviour. Furthermore, the model is able to predict onset of blocked flow nearly perfectly three to five days ahead in many of the major cases. The forecasts that capture the onset remained in the blocked flow regime throughout the forecast range. Beyond a forecast time of three to five days, only a small fraction of the ensemble members entered the blocked flow state while the remainder of the ensemble members stayed in the non-blocked flow state. Therefore, we found that there exists a limit, in the middle of the medium range, beyond which forecasts of blocking onsets are to be considered primarily as probabilistic. This behaviour is not consistent with a linear reasoning. On the contrary it is indeed what we would expect from a system governed by a double-well pseudo-potential.

Acknowledgments

The authors wish to thank Branko Grisogono, Jenny Brandefelt and Fabio D'Andrea for several valuable comments and Måns Håkansson for technical support. NCEP reanalysis data were provided by the National Oceanic and Atmospheric Administration–Cooperative Institute for Research in Environmental Sciences (NOAA–CIRES) Climate Diagnostics Center, Boulder, CO, USA, from their web site at http://www.cdc.noaa.gov/. ECMWF Ensemble Prognosis System forecasts and analysis for the winter 2000–2001 were provided by the ECMWF, Reading, UK.

References

Berggren, R., Bolin, B. and Rossby, C.-G. 1949. An aerological study of zonal motion, its perturbations and break-down. *Tellus* **1**, 14–37.

Buizza, R. and Palmer, T. N. 1995. The singular-vector structure of the atmospheric global circulation. *J. Atmos. Sci.* **52**, 1434–1456.

Charney, J. G. and DeVore, J. G. 1979. Multiple flow equilibria in the atmosphere and blocking. *J. Atmos. Sci.* **36**, 1205–1216.

Chen, W. Y. and Juang, H.-M. H. 1992. Effects of transient eddies on blocking flows: general circulation model experiments. *Mon. Wea. Rev.* **120**, 787–801.

D'Andrea, F., Tibaldi, S., Blackburn, M., Boer, G., Déqué, M., Dix, M. R., Dugas, B., Ferranti, L., Iwasaki, T., Kitoh, A., Pope, V., Randall, D., Roeckner, E., Strauss, D., Stern, W., Van den Dool, H. and Williamson, D. 1998. Northern Hemsiphere atmospheric blocking as simulated by 15 atmospheric general circulation models in the period 1979–1988. *Climate Dyn.* **14**, 385–407.

Ditlevsen, P. D. 1999. Anomalous jumping in a double-well potential. *Phys. Rev. E* **60**, 172–179.

Dole, R. M. and Gordon, N. D. 1983. Persistent anomalies of the extratropical Northern Hemisphere wintertime circulation: geographical distribution and regional persistence characteristics. *Mon. Wea. Rev.* **111**, 1567–1586.

Ferranti, L., Klinker, E., Hollingsworth, A. and Hoskins, B. J. 2002. Diagnosis of systematic forecast errors dependent on flow pattern. *Q. J. R. Meteor. Soc.* **128**, 1623–1640.

Held, I. M. 1983. Stationary and quasi-stationary eddies in the extratropical troposphere: theory. In *Large-Scale Dynamical Processes in the Atmosphere*, Academic Press, New York, 127–168.

Holton, J. R. 1992. *An Introduction to Dynamic Meteorology*, 3rd edition. Academic Press, Seattle, WA, 510 pp.

Hoskins, B. J. and Karoly, D. J. 1981. The steady linear response of a spherical atmosphere to thermal and orographic forcing. *J. Atmos. Sci.* **38**, 1179–1196.

Hoskins, B. J., Buizza, R. and Badger, J. 2000. The nature of singular vector growth and structure. *Q. J. R. Meteor. Soc.* **126**, 1565–1580.

Itoh, H. and Kimoto, M. 1996. Multiple attractors and chaotic itinerancy in a quasi-geostrophic model with realistic topography: implications for weather regimes and low-frequency variability. *J. Atmos. Sci.* **53**, 2217–2231.

Källén, E. 1981. Nonlinear effects of orographic and momentum forcing in a low-order, barotropic model. *J. Atmos. Sci.* **38**, 2150–2163.

Källén, E. 1985. On hysteresislike effects in orographically forced models. *Tellus* **37**A, 249–257.

Legras, B. and Ghil, M. 1985. Persistent anomalies, blocking and variations in atmospheric predictability. *J. Atmos. Sci.* **42**, 433–471.

Lejenäs, H. and Økland, H. 1983. Characteristics of Northern Hemispheric blocking as determined from a long time series of observational data. *Tellus* **35**A, 350–362.

Michelangeli, P.-A. and Vautard, R. 1998. The dynamics of Euro-Atlantic blocking onsets. *Q. J. R. Meteor. Soc.* **124**, 1045–1070.

Molteni, F., Buizza, R., Palmer, T. N. and Petroliagis, T. 1996. The ECMWF Ensemble Prediction System: methodology and validation. *Q. J. R. Meteor. Soc.* **122**, 73–120.

Palmer, T. N., Brankovic, C., Molteni, F. and Tibaldi, S. 1990. Extended-range predictions with ECMWF models: Interannual variability in operational model integrations. *Q. J. R. Meteor. Soc.* **116**, 799–834.

Pavan, V., Tibaldi, S. and Brankovich, C. 2000. Seasonal prediction of blocking frequency: results from winter ensemble experiments. *Q. J. R. Meteor. Soc.* **126**, 2125–2142.

Reinhold, B. and Pierrehumbert, R. 1982. Dynamics of weather regimes: quasi-stationary waves and blocking. *Mon. Wea. Rev.* **110**, 1105–1145.

Rex, D. F. 1950a. Blocking action in the Middle Troposphere and its effect upon regional climate (I). An aerological study of blocking. *Tellus* **2**, 196–211.

Rex, D. F. 1950b. Blocking action in the Middle Troposphere and its effect upon regional climate (II). The climatology of atmospheric blocking. *Tellus* **2**, 275–301.

Rex, D. F. 1951. The effect of Atlantic blocking action upon European climate. *Tellus* **3**, 100–112.

Simmons, A. J., Mureau, R. and Petroliagis, T. 1995. Error growth and estimates of predictability from the ECMWF forecasting system. *Q. J. R. Meteor. Soc.* **121**, 1739–1771.

Tibaldi, S. and Molteni, F. 1990. On the operational predictability of blocking. *Tellus* **42A**, 343–365.

Tibaldi, S., Tosi, E., Navarra, A. and Pedulli, L. 1994. Northern and Southern hemisphere seasonal variability of blocking frequency and predictability. *Mon. Wea. Rev.* **122**, 1971–2003.

Tibaldi, S., Ruti, P., Tosi, E. and Maruca, M. 1995. Operational predictability of winter blocking at ECMWF: an update. *Ann. Geophys.* **13**, 305–317.

Trevisan, A., Pancotti, F. and Molteni, F. 2001. Ensemble prediction in a model with flow regimes. *Q. J. R. Meteor. Soc.* **127**, 343–358.

Wallace, J. M. and Gutzler, D. S. 1981. Teleconnections in the geopotential height field during the Northern Hemisphere winter. *Mon. Wea. Rev.* **109**, 784–812.

Yang, S., Reinhold, B. and Källén, E. 1997. Multiple weather regimes and baroclinically forced spherical resonance. *J. Atmos. Sci.* **54**, 1397–1409.